

# Assembly of Helicene-Capped N,P,N,P,N-Helicands within Cu<sup>I</sup> Helicates: Impacting Chiroptical Properties by Ligand–Ligand Charge Transfer\*\*

Volodimir Vreshch, Mehdi El Sayed Moussa, Brigitte Nohra, Monika Srebro, Nicolas Vanthuyne, Christian Roussel, Jochen Autschbach,\* Jeanne Crassous,\* Christophe Lescop,\* and Régis Réau\*

In memory of Christian G. Claessens

Helical derivatives are fascinating structures that have sparked the imagination of chemists and continue to motivate an intensive and creative synthetic effort. Helicates and helicenes are two prototypical helical structures in molecular chemistry.<sup>[1]</sup> Since their introduction by Lehn et al.,<sup>[2a–e]</sup> there has been interest in helicates and their potential applications such as functional chiral supramolecular assemblies,<sup>[2c–e]</sup> efficient chiral emitters,<sup>[2f]</sup>  $\alpha$ -helices mimics, and antimicrobial agents.<sup>[1b]</sup> Their syntheses generally imply the use of multidentate ligands named helicands, whose coordination mode exhibits atropisomeric chirality.<sup>[2a–e]</sup> These helicands are mainly based on pyridyl-type or related N-donors and very rarely on phosphorous-based ligands.<sup>[3]</sup> Helicenes are intriguing organic derivatives that combine a helical backbone and a  $\pi$ -conjugated system.<sup>[4]</sup> This unique skeleton endows helicenes with chiroptical properties that are of great interest to many fields (catalysis, material sciences, and others).

Herein, we describe the first helicates built on helicene-containing helicands. Their double-stranded skeleton results from the close assembly on metal-dimers of pentadentate phosphole-pyridine helicands exhibiting original coordination modes. A chiral transfer from the helicene-helicand to the helicate skeleton gave enantiopure complexes. Their chiral properties were elucidated following experimental and theoretical study, which revealed intriguing helicand–helicate charge transfer that impacts the chiroptical properties of these assemblies.

2,5-Bis(2-pyridyl)phosphole **A** can act as an N,P-chelate, or as an N,P,N-pincer with a very rare bridging  $\mu$ -P donor, stabilizing a variety of Cu<sup>I</sup>-dimers (Figure 1 a).<sup>[5]</sup> To combine these two coordination behaviors into one heteroditopic ligand, the coordination chemistry of **2a** (Figure 1 a) featuring

[\*] Dr. V. Vreshch, M. El Sayed Moussa, Dr. B. Nohra, Dr. J. Crassous, Dr. C. Lescop, Prof. R. Réau  
Sciences Chimiques de Rennes UMR 6226 CNRS  
Université de Rennes 1, 35042 Rennes Cedex (France)  
E-mail: jeanne.crassous@univ-rennes1.fr  
christophe.lescop@univ-rennes1.fr  
regis.reau@univ-rennes1.fr

Dr. M. Srebro, Prof. J. Autschbach  
Department of Chemistry, University at Buffalo  
State University of New York, Buffalo, NY 14260 (USA)  
and

Department of Theoretical Chemistry, Faculty of Chemistry  
Jagiellonian University, 30-060 Krakow (Poland)  
E-mail: jochena@buffalo.edu

Dr. N. Vanthuyne, Prof. C. Roussel  
Chirosciences, UMR 7313, Stéréochimie Dynamique et Chiralité  
Aix-Marseille University, 13397 Marseille (France)

[\*\*] Financial supports: V.V. thanks the “Région Bretagne” for a CREATE fellowship. Financial support from the CNRS, University of Rennes 1, ANR (12-BS07-0004-METALHEL-01) and the National Science Foundation (CHE 0952253). J.A. and M.S. thank the Center for Computational Research (CCR) at the University at Buffalo. M.S. acknowledges the Foundation for Polish Science (“START” stipend for young researchers) and the Ministry of Science and Higher Education in Poland (“Mobility Plus” program).

Supporting information for this article (experimental and computational details) is available on the WWW under <http://dx.doi.org/10.1002/anie.201207251>.

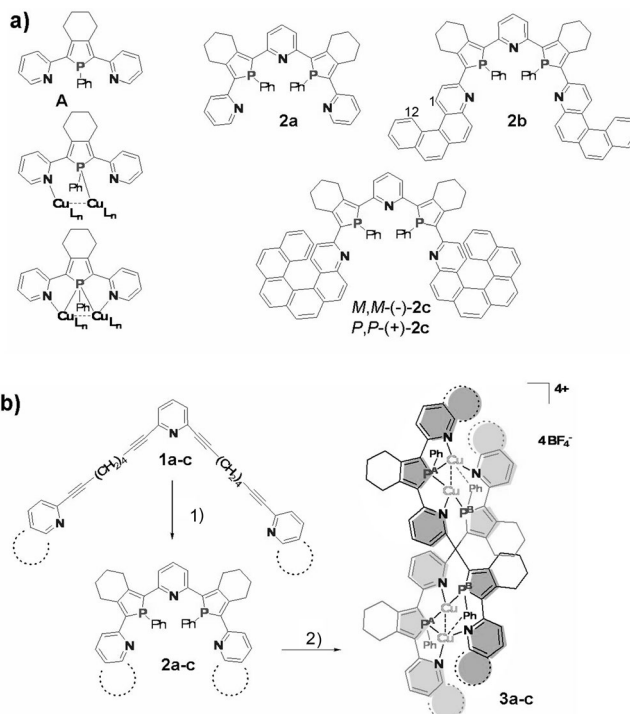


**Figure 1.** a) Ligands **A** and **2a–c**; b) syntheses of **3a–c**. 1) 2 equiv  $[\text{Cp}_2\text{ZrCl}_2]$ , 4 equiv  $n\text{BuLi}$ , tetrahydrofuran, 40 °C, 2 equiv  $\text{PhPBr}_2$ ; 2) 2 equiv  $[\text{Cu}(\text{CH}_3\text{CN})_4]\text{BF}_4$ , RT,  $\text{CH}_2\text{Cl}_2$ .

an N,P,N,P,N-core was investigated. This novel derivative was prepared from bis-diyne **1a** using the Fagan–Nugent route (Figure 1b).<sup>[6]</sup> Compound **2a** was isolated as an air-stable yellow powder (87 % yield) and characterized by high-resolution mass spectrometry, elemental analysis, and multinuclear NMR spectroscopy.<sup>[7]</sup> A variable temperature <sup>31</sup>P{<sup>1</sup>H} NMR spectroscopy study showed that a fast inversion of the two stereogenic P-centers of **2a** ( $\delta$ , +11.9 and +12.0 ppm) takes place at room temperature (RT), with a classic inversion barrier for phosphole (16 kcal mol<sup>-1</sup>; Supporting Information, Figure S1),<sup>[6]</sup> resulting in an equilibrium between the two *meso* (*R<sub>P</sub>S<sub>P</sub>*) and *rac* (*R<sub>P</sub>R<sub>P</sub>/S<sub>P</sub>S<sub>P</sub>*) diastereomers.<sup>[8]</sup> Note that this low inversion barrier, which sets phospholes apart from usual phosphines (inversion barrier, ca. 30–35 kcal mol<sup>-1</sup>), is a way to obtain stereoselective coordination of these P-heteroles with metal ions.<sup>[9]</sup> The *rac*-diastereoisomer was characterized by an X-ray diffraction study (Figure 2a).<sup>[7]</sup> Its metric parameters (including torsion angles between the heterocycles) are very similar to those of ligand **A** (Table S3). The presence of an extended  $\pi$ -conjugated system within **2a** was shown by a strong UV/Vis absorption band with a  $\lambda_{\text{max}}$  at 385 nm (Figure S8).

Derivative **2a** was reacted at RT in CH<sub>2</sub>Cl<sub>2</sub> with two equivalents of [Cu(CH<sub>3</sub>CN)<sub>4</sub>]BF<sub>4</sub> affording, after purification by crystallization, the tetrametallic complex [Cu<sub>4</sub>(**2a**)<sub>2</sub>](BF<sub>4</sub>)<sub>4</sub> **3a** (Figure 1b).<sup>[7]</sup> This complex was isolated as an air-stable orange polycrystalline powder in 66 % yield. Its <sup>31</sup>P{<sup>1</sup>H} NMR spectrum recorded in CD<sub>2</sub>Cl<sub>2</sub> at RT exhibits a well-defined AB system ( $\delta$ , -3.4 and -6.4 ppm, <sup>2</sup>J<sub>pp</sub> = 125.0 Hz, Figure 2b). These signals are shifted to low frequency compared to those of **2a** clearly indicating the coordination of the two P-centers onto the Cu<sup>I</sup> ions. The room temperature <sup>1</sup>H NMR spectrum of **3a** displays one single set of sharp signals and reveals that the two P–Ph moieties and the two terminal pyridine groups are not equivalent. One of these two P–Ph groups bears magnetically non-equivalent H<sub>ortho</sub> and H<sub>meta</sub> atoms, suggesting that there is hindered rotation about this P–Ph bond, associated with an unsymmetrical environment.

Overall, the simplicity of the NMR spectra suggests a stereoselective coordination process of **2a** on the Cu<sup>I</sup> ions, as observed for related (2-pyridyl)phosphole P,N-donors.<sup>[9]</sup> An X-ray diffraction study<sup>[7]</sup> revealed that derivative **3a** is a *pseudo* C<sub>2</sub>-symmetric,<sup>[10]</sup> tetracationic complex (Figure 2b) resulting from the coordination of two *meso*-N,P,N,P,N-ligands **2a**<sup>[8]</sup> on two Cu<sup>I</sup> dimers. For each ligand **2a**, one N,P,N-moiety acts as a six-electron  $\mu$ -1 $\kappa$ N:1,2 $\kappa$ P:2 $\kappa$ N donor with a bridging P-center (d(P–Cu), 2.35  $\pm$  0.05 Å) towards one Cu<sup>I</sup> dimer (P<sup>A</sup>, Figure 1b, 2b), and one P,N-moiety acts as a four-electron  $\mu$ -1 $\kappa$ N:2 $\kappa$ P donor on the second Cu<sup>I</sup> dimer (P<sup>B</sup>, Figure 1b, 2b). Therefore, the two possible coordination behaviors of ligand **A** (P,N- or N,P,N-donors with a  $\mu$ -P, Figure 1a) are found for the pentadendate N,P,N,P,N-donor **2a**. As is usually observed for Cu<sup>I</sup> dimers stabilized by  $\mu$ -1 $\kappa$ N:1,2 $\kappa$ P:2 $\kappa$ N ligand **A**, the phosphole and pyridine heterocycles are slightly twisted (P–C–C–N, 25  $\pm$  5°) and the metal–metal distance is short (ca. 2.6 Å, Table S4) suggesting the presence of d<sup>10</sup>–d<sup>10</sup> metallophilic interactions.<sup>[5a,b]</sup> Note that an interaction appears to take place between one Cu<sup>I</sup> center and the C<sub>ipso</sub> atom of the P<sup>B</sup>–Ph, based on the short d(Cu–C<sub>ipso</sub>) contacts (2.362(4) Å and 2.455(4) Å, Figure 2b). A Bader analysis showed a bond-critical point for both contacts. A natural bond orbital (NBO) analysis did, however, not indicate a pronounced covalent character, revealing a weak  $\pi$ -interaction between the metal center and the phenyl ring (donation from a  $\pi$ (C<sub>ipso</sub>C<sub>ortho</sub>)- to a 4s(Cu)-centered orbital and back-donation of a Cu lone-pair into a  $\pi^*$ (C<sub>ipso</sub>C<sub>ortho</sub>) orbital). Remarkably, the two N,P,N,P,N-ligands **2a** wrap around the Cu<sup>I</sup> dimers, defining a double-stranded helical array, as shown by dihedral angles (DA) of approximately +60° between the N,P-chelate and the N,P,N-chelate mean planes (Figure 2b). In fact, upon coordination of the Cu<sup>I</sup> dimers, the **2a** ligands become *tropos*,<sup>[11]</sup> and are homochiral within the assembly **3a**.<sup>[8]</sup> It is important to note that this solid-state structure is in agreement with the multinuclear NMR data recorded in solution. The <sup>31</sup>P{<sup>1</sup>H} NMR AB system (Figure 2b) results from the presence of two non-equivalent

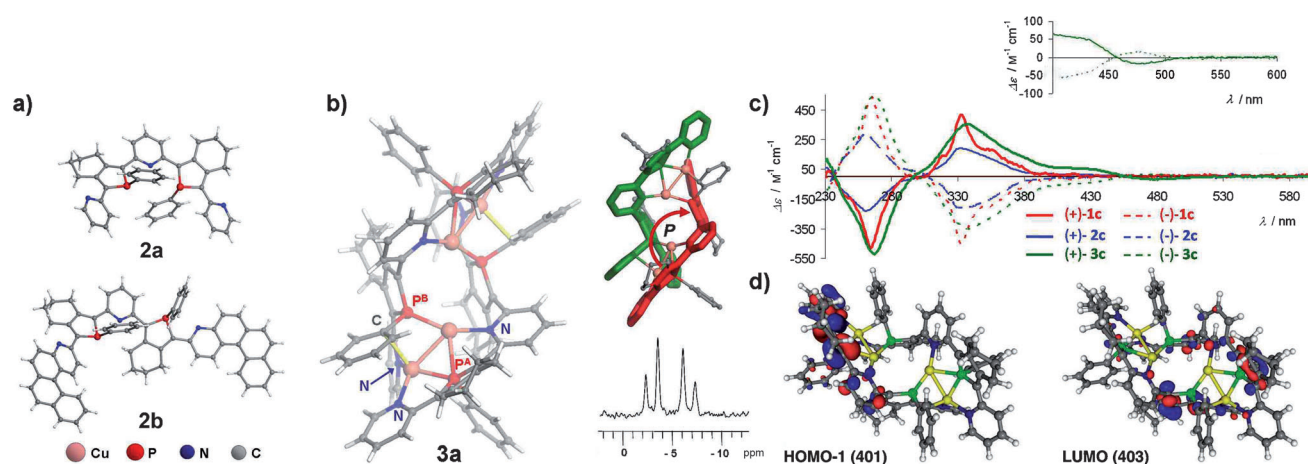


**Figure 2.** a) X-ray crystallographic structures of **2a**, b) X-ray crystallographic structure (left, the Cu–C interaction is highlighted in yellow), schematic view of the wrapping of the ligands around the metal dimers (top, right), and <sup>31</sup>P{<sup>1</sup>H} NMR spectrum (bottom, right) for **3a**; c) CD spectra of bis-diynes **1c**, ligand **2c**, and helicate **3c** enantiomers. Insert: low-energy CD-active bands of **3c**; d) Selected MOs of helicate **3a** involved in the CD-active bands.

P-centers, while the  $\text{Cu}^{\text{I}}\text{-C}_{\text{ipso}}\text{C}_{\text{ortho}}$   $\pi$ -interaction rationalizes the observation of non-equivalent  $\text{H}_{\text{ortho}}$  and  $\text{H}_{\text{meta}}$  protons for one P–Ph moiety (see above). The  $^{31}\text{P}\{^1\text{H}\}$  NMR spectra is essentially unchanged between RT and 241 K (Figure S6), showing that exchange reactions do not take place or are slow in solution on the NMR time scale.<sup>[12]</sup> Therefore, the NMR data of **3a** give an unambiguous signature of the formation of the  $[(\text{Cu}^{\text{I}})_4(\mathbf{2a})_2]$  helicate backbone.

The structure of complex **3a** displays several original aspects. It is the first example of a double-stranded helicate derivative built on heterotopic *tropos* N,P-helicands. Furthermore, these N,P-helicands feature  $\mu$ -P donors, a rare coordination mode for phosphine donors.<sup>[5]</sup> Another important feature is that the  $\lambda_{\text{max}}$  of complex **3a** is similar to that of the free ligand **2a**, with the  $\lambda_{\text{onset}}$  being red-shifted by 60 nm (Figure S9), indicating significant conjugation within the coordinated  $\pi$ -frameworks. Furthermore, the fact that the N,P,N,P,N-donor **2a** adopts a stable conformation upon coordination can be exploited to readily generate structural diversity in helicate chemistry. For example, ligand **2a** reacted at RT in  $\text{CH}_2\text{Cl}_2$  with 1.5 equivalents of  $\text{AgBF}_4$  giving rise to a novel helicate  $[\text{Ag}_3(\mathbf{2a})_2](\text{BF}_4)_2$  (**4a**, Figure S7) based on an almost equilateral triangle  $\text{Ag}_3$  core (internal angle,  $57.9^\circ$ – $61.3^\circ$ ) with short metal–metal distances (ca. 2.8 Å).<sup>[7]</sup> This  $\text{Ag}_3$  core is stabilized by two *tropos rac*-ligands **2a**<sup>[8]</sup> that wind around the trimetallic  $\text{Ag}_3$  unit (Figure S7).

We then explored the enantiomeric resolution of *P,P*- and *M,M*-**3a** helicate assemblies. However, all attempts to resolve the diastereomeric (**3a**<sup>4+</sup>,  $\Delta\text{A-TRISPHAT}^-$ ) mixture by crystallization failed.<sup>[12]</sup> Another strategy exploiting the highly stereoselective coordination process of ligand **2a** on  $\text{Cu}^{\text{I}}$  dimers was therefore devised. We investigated whether a chiral transfer process may occur with derivative **2c** (Figure 1a), which has the N,P,N,P,N-core of **2a** and is functionalized with enantiopure aza[6]helicene termini. It was expected that a chiral transfer from the aza[6]helicene to the N,P,N,P,N-core could take place during the stereoselective coordination process on  $\text{Cu}^{\text{I}}$  dimers, affording **2c** with an enantiopure helical *meso*-configuration.<sup>[8]</sup> This was a unique opportunity to study the possible chiral transfer from the peripheral helicene moieties to the helicate core within a single assembly, to obtain molecules with an unprecedented chiral topology. Because the aza[6]helicene fragments are rather bulky substituents, a model ligand **2b** with aza[4]helicene termini (Figure 1a) was first used to probe both the ligand synthetic method and the supramolecular synthetic strategy towards helicene-containing helicates. The Fagan–Nugent route was applied to diyne **1b** (Figure 1b) and, following purification by column chromatography, the air-stable derivative **2b** (Figure 1a) was isolated in 30% yield.<sup>[7]</sup> The multinuclear NMR data from this compound support the proposed structure. For example, the  $^1\text{H}$  NMR of **2b** displays characteristic signals at 8.84 ppm and 9.15 ppm for the aza[4]helicene  $\text{H}^1$  and  $\text{H}^{12}$  protons (Figure 1a), respectively. The  $^{31}\text{P}\{^1\text{H}\}$  NMR spectrum (RT,  $\text{CD}_2\text{Cl}_2$ , Figure S2) displays two singlets of similar intensities at +11.9 ppm and +12.1 ppm, as observed for derivative **2a**, due to the rapid racemization processes of both the [4]-helicene and phosphole (inversion at P,  $\Delta G^\ddagger \approx 16 \text{ kcal mol}^{-1}$ ) moieties. The X-

ray crystallographic study<sup>[7]</sup> of the *rac* diastereoisomer of **2b** (Figure 2a) showed that its N,P,N,P,N-core has the same structural characteristics as **2a** (Table S3). The torsion angles (below  $31^\circ$ ) between the heterocycles of **2b** allow efficient  $\pi$ -conjugation throughout the molecule, as shown by the red-shift of its  $\lambda_{\text{max}}$  compared to **2a** ( $\Delta\lambda_{\text{max}}$ , 30 nm; Figure S8). Note that derivative **2b** is the longest phosphole-based  $\pi$ -conjugated system characterized by X-ray diffraction to date.<sup>[6b]</sup> Treatment of **2b** with  $[\text{Cu}(\text{CH}_3\text{CN})_4]\text{BF}_4$  in the reaction conditions used to prepare **3a** afforded a novel complex **3b**, which was isolated in 55% yield as an air-stable red solid (Figure 1b). Its  $^{31}\text{P}\{^1\text{H}\}$  NMR spectroscopic data are very similar to those of complex **3a** ( $\delta$ ,  $-3.7$  and  $-7.5$  ppm,  $^2J_{\text{PP}} = 123.3 \text{ Hz}$ , Figure S5) showing the formation of a  $[(\text{Cu}^{\text{I}})_4(\mathbf{2b})_2]$  helicate backbone. These results validate our strategy and the synthesis of the enantiopure *P,P*- and *M,M*-[6]helicene ligand **2c** (Figure 1a) was therefore undertaken. The bis-diyne precursor **1c** (Figure 1b) was prepared using a series of Sonogashira couplings performed on enantiopure aza[6]helicene synthons resolved by semi-preparative enantiomeric HPLC separation (*ee* > 99%).<sup>[7]</sup> Its UV/Vis spectrum shows absorption bands between 300–370 nm corresponding to the  $\pi$ – $\pi^*$  transitions of the helicene fragments and two maxima at 410 nm and 440 nm. Compound *P,P*-**1c** displays a strong negative circular dichroism (CD)-active band at 263 nm ( $\Delta\epsilon = -484 \text{ M}^{-1} \text{ cm}^{-1}$ , Figure 2c) and a strong positive band at 331 nm ( $\Delta\epsilon = 399 \text{ M}^{-1} \text{ cm}^{-1}$ ), together with a high molar rotation (MR) value at 589 nm ( $[\phi]_{\text{D}}^{23} = \pm 20500 (\pm 5\%)^\circ \text{ cm}^2 \text{ dmol}^{-1}$ ,  $\text{CH}_2\text{Cl}_2$ ,  $c = 1 \times 10^{-4} \text{ M}$ ). The corresponding *P,P*-(+)- and *M,M*-(-)-derivatives **2c** were subsequently prepared in a moderate yield (50%) using the Fagan–Nugent route (Figure 1b).<sup>[7]</sup> The  $^{31}\text{P}\{^1\text{H}\}$  NMR spectrum of the (-)-**2c** enantiomer at 298 K reveals the existence of a complex stereoisomeric mixture in solution owing to the presence of the stereogenic P-centers. However, this  $^{31}\text{P}\{^1\text{H}\}$  NMR spectrum is greatly simplified upon increasing the temperature, and at 318 K, only two signals similar to those recorded for **2a,b** are observed (Figure S3). The optical (UV/Vis, CD) and MR signatures of **2c** are typical<sup>[9]</sup> for a molecule with an extended phosphole-based  $\pi$ -conjugated system bearing two helicene moieties.<sup>[7]</sup> As a result of the complex epimeric mixture, the mirror-image CD spectra of (+)- and (-)-**2c** show CD bands with lower intensity than those of **1c** (Figure 2c). Enantiomerically pure (+)- and (-)-N,P,N,P,N-ligands **2c** were reacted with 2 equiv of  $[\text{Cu}(\text{CH}_3\text{CN})_4]\text{BF}_4$  at RT in  $\text{CH}_2\text{Cl}_2$  affording complexes (+)- and (-)-**3c** (approximately 60% yield) as intensely red-colored solids (Figure 1b).<sup>[7]</sup> The  $^{31}\text{P}\{^1\text{H}\}$  NMR spectrum of (+)/(-)-**3c** displays the typical *AB* system ( $-3.7$  and  $-7.4$  ppm,  $^2J_{\text{PP}} = 123.9 \text{ Hz}$ , Figure S5) observed for derivatives **3a,b**, showing the formation of a helicate core similar to that of **3a** (Figure 2b). The simplicity of this  $^{31}\text{P}\{^1\text{H}\}$  NMR spectrum contrasts with the complexity of that of the free ligand **2c** and shows that, as observed with the model helicands **2a,b**, the coordination of the N,P,N,P,N-core of **2c** on the  $\text{Cu}^{\text{I}}$ -dimers is highly stereoselective. Note that the low-energy part of the UV/Vis spectrum of **3c** is essentially comparable to that of **3b** (Figure S9). The fact that helicands **2c** become *tropos* upon coordination has an important impact on its CD spectra.



Complexes (+)/(−)-**3c** display much more intense CD bands than those of (+)/(−)-**2c** ((+)-**2c**:  $\Delta\epsilon = -228\text{ M}^{-1}\text{ cm}^{-1}$  at 260 nm and  $+187\text{ M}^{-1}\text{ cm}^{-1}$  at 330 nm; (+)-**3c**:  $\Delta\epsilon = -514\text{ M}^{-1}\text{ cm}^{-1}$  at 266 nm and  $+349\text{ M}^{-1}\text{ cm}^{-1}$  at 337 nm, Figure 2c) and new CD-active bands of moderate magnitude between 400–600 nm appeared ((+)-**3c**:  $\Delta\epsilon = +59\text{ M}^{-1}\text{ cm}^{-1}$  at 410 nm and  $-17\text{ M}^{-1}\text{ cm}^{-1}$  at 480 nm). The MR values of (+)/(−)-**3c** are very high ( $[\phi]_{\text{D}}^{23} = \pm 21\,000(\pm 5\%)^{\circ}\text{ cm}^2\text{ dmol}^{-1}$ ,  $\text{CH}_2\text{Cl}_2$ ,  $c = 0.0005$ ). These chiroptical data, along with the  $^{31}\text{P}\{\text{H}\}$  NMR spectroscopic data, strongly support that helicates (+)/(−)-**3c** have been obtained in enantiomerically pure form owing to the stereoselective coordination of helicands (+)/(−)-**2c** with the  $\text{Cu}^{\text{I}}$  dimers.

To investigate the chiroptical properties of these unprecedented structures **3a–c** (Figure 1b), in which two extended  $\pi$ -conjugated organic helicene-containing ligands are closely held together in a helicate framework, TDDFT B3LYP/SV(P) calculations have been carried out.<sup>[7]</sup> The goal was to elucidate the CD signature for the common N,P,N,P,N-helicand moieties within the helicate series **3a–c** (Figure 1b) and to establish the origin of the CD-bands at 400–600 nm appearing upon complexation (metal-ligand charge transfer (MLCT), intra-, or ligand–ligand charge transfer (ILCT and LLCT, respectively)). Complex **3a** was selected for this study since its skeleton consists exclusively of the N,P,N,P,N-helicate core. The calculated CD spectrum of *P*-**3a** displays four main bands, two negative at 240 nm and 343 nm, and two positive at 270 nm and 375 nm (Figure S17). The calculated positive band ( $R = 228 \times 10^{-40}$  cgs) at 375 nm in *P*-**3a** compares well with the experimental positive band around 400 nm observed for **3c** (Figure 2c), suggesting a chiral transfer from the *P*-helicene moieties of **2c** to the *P*-helicate core of **3c**. This result is among the rare examples highlighting the peculiar ability of helicene moieties incorporated within large  $\pi$ -conjugated ligands to efficiently transfer chirality to the metal–ligand core.<sup>[9d]</sup> Furthermore, analysis of dominant excitations in terms of individual molecular orbital pairs (MOs; Table S6, and Figures S19, S20) reveals that no MLCT takes place and that the overall involvement of the Cu atom MOs in all the CD-active bands is negligible. Therefore, the  $\text{Cu}^{\text{I}}$  dimers do not electronically impact the chiroptical property of these novel  $\pi$ -conjugated helicate structures **3a–c**. Their role is to assemble ligands **2a–c** and to freeze their conformation upon an original coordination mode involving both their N, $\mu$ -P,N- and P,N-moieties. The low energy CD-active bands show signatures of ILCT and LLCT. For example, in **3a**, two excitations contribute to the CD band of lowest energy, number 1 of almost vanishing strength and number 2 of dominant rotatory strength (Figure S17 and Table S6). These involve nearly degenerate HOMO and HOMO-1 for number 1 and number 2, respectively, and nearly degenerate LUMO+2 and LUMO+3 as well as LUMO and LUMO+1 orbitals (Figure 2d). HOMO-1 and HOMO (MOs number 401, 402; Figure S19) have electronic density each localized on one part of the *P*-**2a** ligand, but linear combinations may be taken where, similar to LUMO+2 and LUMO+3 (MOs number 405, 406; Figure S20), electronic density extends over parts of both ligands. Note that LLCT is also involved in many other transitions with high

rotatory strength values. This theoretical study clearly reveals that the original structure of complexes **3a–c**, in which two helicands are closely held together by way of coordination on electronically innocent metal dimers, allows both ILCT and LLCT to take place, resulting in high chiroptical activity.

In conclusion, helicene and helicate chemistry have been combined using molecular engineering of an N,P,N,P,N-core based on phosphole rings, which become *tropos* upon coordination. This approach, relying on the coordination-driven close assembly of two helicene-capped helicands, opens interesting perspectives because it allows structural diversity to be created by varying the metal ion and the preparation of helicates with strong chiroptical properties arising from LLCT.

Received: September 7, 2012

Revised: November 9, 2012

Published online: January 10, 2013

**Keywords:** chiro-optical properties · coordination chemistry · density functional calculations · helicates · helicenes

- [1] For recent examples, see: helicates a) J.-F. Ayme, J. E. Beves, D. A. Leigh, R. T. McBurney, K. Rissanen, D. Schultz, *Nat. Chem.* **2012**, *4*, 15–20; b) S. E. Howson, A. Bolhuis, V. Brabec, G. J. Clarkson, J. Malina, A. Rodger, P. Scott, *Nat. Chem.* **2012**, *4*, 31–36; c) W. Xuan, Y. Liu, Z. Chen, Y. Cui, *J. Am. Chem. Soc.* **2012**, *134*, 6904–6907; d) J.-F. Ayme, J. E. Beves, D. A. Leigh, R. T. McBurney, K. Rissanen, D. Schultz, *J. Am. Chem. Soc.* **2012**, *134*, 9488–9497; helicenes e) L. Severa, M. Ončák, D. Koval, R. Pohl, D. Šaman, I. Čisárová, P. E. Reyes-Gutiérrez, P. Sázelová, V. Kašička, F. Teplý, P. Slavíček, *Angew. Chem.* **2012**, *124*, 12138–12142; *Angew. Chem. Int. Ed.* **2012**, *51*, 11972–11976; f) A. Ueda, H. Wasa, S. Suzuki, K. Okada, K. Sato, T. Takui, Y. Morita, *Angew. Chem.* **2012**, *124*, 6795–6799; *Angew. Chem. Int. Ed.* **2012**, *51*, 6691–6695; g) K. Yavari, S. Moussa, B. Ben Hassine, P. Retailleau, A. Voituriez, A. Marinetti, *Angew. Chem.* **2012**, *124*, 6852–6856; *Angew. Chem. Int. Ed.* **2012**, *51*, 6748–6752; h) E. Anger, M. Srebro, N. Vanthuyne, L. Toupet, S. Rigaut, C. Roussel, J. Autschbach, J. Crassous, R. Reau, *J. Am. Chem. Soc.* **2012**, *134*, 15628–15631.
- [2] a) J.-M. Lehn, A. Rigault, J. Siegel, J. Harrowfield, B. Chevrier, D. Moras, *Proc. Natl. Acad. Sci. USA* **1987**, *84*, 2565–2569; b) For a recent review on helicate synthesis: S. E. Howson, P. Scott, *Dalton Trans.* **2011**, *40*, 10268–10277; c) J.-M. Lehn, *Supramolecular Chemistry: Concepts and Perspectives*, VCH, Weinheim, **1995**, Chap. 9; d) C. Piguet, G. Bernardinelli, G. Hopfgartner, *Chem. Rev.* **1997**, *97*, 2005–2062; e) M. Albrecht, *Chem. Rev.* **2001**, *101*, 3457–3497; f) F. Stomeo, C. P. Lincheneau, J. P. Leonard, J. E. O'Brien, R. D. Peacock, C. P. McCoy, T. Gunnlaugsson, *J. Am. Chem. Soc.* **2009**, *131*, 9636–9637.
- [3] Selected examples: a) P. K. Bowyer, V. C. Cook, N. Gharib-Naseri, P. A. Gugger, A. D. Rae, G. F. Swiegers, A. C. Willis, J. Zank, S. B. Wild, *Proc. Natl. Acad. Sci. USA* **2002**, *99*, 4877–4882; b) C. J. Blake, V. C. Cook, M. A. Keniry, H. J. Kitto, A. D. Rae, G. F. Swiegers, A. C. Willis, J. Zank, S. B. Wild, *Inorg. Chem.* **2003**, *42*, 8709–8715; c) S. L. James, *Chem. Soc. Rev.* **2009**, *38*, 1744–1758.
- [4] a) T. J. Katz, *Angew. Chem.* **2000**, *112*, 1997–1999; *Angew. Chem. Int. Ed.* **2000**, *39*, 1921–1923; b) A. Urbano, *Angew. Chem.* **2003**, *115*, 4116–4119; *Angew. Chem. Int. Ed.* **2003**, *42*, 3986–3989; c) A. Rajca, M. Miyasaka in *Functional Organic Materials* (Eds.: T. J. J. Müller, U. H. F. Bunz), Wiley-VCH,

- Weinheim, **2007**, pp. 543–577; d) Y. Shen, C. F. Chen, *Chem. Rev.* **2012**, *112*, 1463–1535.
- [5] a) F. Leca, C. Lescop, E. Rodriguez-Sanz, K. Costuas, J.-F. Halet, R. Réau, *Angew. Chem.* **2005**, *117*, 4436–4439; *Angew. Chem. Int. Ed.* **2005**, *44*, 4362–4365; b) B. Nohra, E. Rodriguez-Sanz, C. Lescop, R. Réau, *Chem. Eur. J.* **2008**, *14*, 3391–3403; c) S. Welsch, B. Nohra, E. V. Peresypkina, C. Lescop, M. Scheer, R. Réau, *Chem. Eur. J.* **2009**, *15*, 4685–4703; d) B. Nohra, S. Graule, C. Lescop, R. Réau, *J. Am. Chem. Soc.* **2006**, *128*, 3520–3521; e) Y. Yao, W. Shen, B. Nohra, C. Lescop, R. Réau, *Chem. Eur. J.* **2010**, *16*, 7143–7163.
- [6] a) R. Réau, T. Baumgartner, *Chem. Rev.* **2006**, *106*, 4681–4727; b) J. Crassous, C. Lescop, R. Réau in *Phosphorus compounds: advanced tools in catalysis and material sciences*, Catalysis by Metal Complexes, *37*, 11, 1st ed., (Eds. M. Peruzzini, L. Gonsalvi), Springer, London, **2011**, p.367.
- [7] For experimental data and computational details, see the Supporting Information.
- [8] The *meso/rac* descriptors refer to the stereochemistry of the phosphorus centers and the *P/M* descriptors refer to the helicands and helicate stereochemistry. An angle of approximately +60° defines the *P* stereochemistry for the *tropos* helicand **2a**. Both *P,P*- and *M,M*-helicates are present in the centrosymmetric crystals.
- [9] a) S. Graule, M. Rudolph, N. Vanthuyne, J. Autschbach, C. Roussel, J. Crassous, R. Réau, *J. Am. Chem. Soc.* **2009**, *131*, 3183–3185; b) S. Graule, M. Rudolph, W. Shen, J. A. G. Williams, C. Lescop, J. Autschbach, J. Crassous, R. Réau, *Chem. Eur. J.* **2010**, *16*, 5976–6005; c) W. Shen, S. Graule, J. Crassous, C. Lescop, H. Gornitzka, R. Réau, *Chem. Commun.* **2008**, 850–853; d) J. Crassous, *Chem. Commun.* **2012**, 48, 9684–9692.
- [10] A short contact interaction between ligands **2a** and one BF<sub>4</sub><sup>−</sup> prevents **3a** (Figure S16) from having an ideal C<sub>2</sub> symmetry. NMR data show that this interaction is not retained in solution.
- [11] a) K. Mikami, K. Aikawa, Y. Yusa, J. J. Jodry, M. Yamanaka, *Synlett* **2002**, 1561–1578; b) K. Mikami, H. Kakuno, K. Aikawa, *Angew. Chem.* **2005**, *117*, 7423–7426; *Angew. Chem. Int. Ed.* **2005**, *44*, 7257–7260.
- [12] One referee suggested that ligand **2a** could exhibit a labile coordination behavior. Note that two sets of signals are observed by <sup>1</sup>H NMR spectroscopy<sup>[7]</sup> upon replacing the BF<sub>4</sub><sup>−</sup> counter anion by Δ-TRISPHAT: a) J. Lacour, C. Ginglinger, F. Favarger, S. Torche-Haldimann, *Chem. Commun.* **1997**, 2285–2286; b) J. Lacour, R. Frantz, *Org. Biomol. Chem.* **2005**, *3*, 15–19, and references therein; c) W. W. N. O, A. J. Lough, R. H. Morris, *Organometallics* **2009**, *28*, 6755–6761; d) R. Zalubovskis, A. Bouet, E. Fjellander, S. Constant, D. Linder, A. Fischer, J. Lacour, T. Privalov, C. Moberg, *J. Am. Chem. Soc.* **2008**, *130*, 1845–1855.